Delft University of Technology

Influence of stiffeners on acoustic emission monitoring of ship structures

Saccone, C.; Pahlavan, Lotfollah

Citation (APA)
Saccone, C., & Pahlavan, L. (2024). Influence of stiffeners on acoustic emission monitoring of ship structures. *e-Journal of Nondestructive Testing*, 1-8. https://doi.org/10.58286/29587

Important note
To cite this publication, please use the final published version (if applicable).
Please check the document version above.

Influence of stiffeners on acoustic emission monitoring of ship structures

Cecilia SACCONE [1], Lotfollah PAHLAVAN [2]

[1] Delft University of Technology, Delft, Netherlands, C.Saccone@tudelft.nl

[2] Delft University of Technology, Delft, Netherlands, L.Pahlavan@tudeflt.nl

Abstract This paper aims to assess propagation of acoustic emission (AE) waves in ship structures in the presence of stiffeners that are commonly present in the structure of ship hulls. The transmission of the ultrasound guided waves and their dependence on the angle of incidence are investigated using spectral finite element (SEM) simulations and experimental measurements. By combining the results of the simulations and experiments, an expression for the transmission coefficient as a function of different angles is presented. The results of this study can be used to maximize the coverage of AE monitoring systems and enhance their sensitivity for the detection of fatigue cracks on ship structures.

Keywords: acoustic emission, ship, stiffener, fatigue, cracks

Introduction

Due to the highly stochastic dynamic loading to which ships are subjected, and the harsh corrosive environments in which they operate, fatigue and corrosion damage can develop in these structures, affecting their structural integrity and remaining lifetime. Fatigue cracks can form in locations that are difficult to detect and/or quantify [1], e.g. intersections of stiffeners with other structural members that are part of the frame of a ship hull, without being detected until they substantially grow. Effective detection of these cracks can mitigate material losses, reducing the risk of operations and environmental damage resulting from failures. Predictive maintenance is crucial to enhance efficiency and operability of ship structures.

Conventional non-destructive techniques (NDT) to assess the structural integrity of ships generally consist of time-consuming, costly and physically demanding procedures. Examples are magnetic particle inspection (MPI), ultrasound testing (UT), and visual inspection both automated and manned [2] [3] [4]. They involve periodic inspections during planned shutdowns, such as dry-docking procedures.

Damage generally changes the response of structures (e.g. mechanical, electromechanical, electromagnetic, etc.). Structural health monitoring (SHM) systems aim at measuring these changes and translating them to the integrity status of the structure [5]. Existing SHM systems take advantage of information about real-time in-service behaviour

[6], differently than periodic inspections. Strain monitoring with long base strain gauges (LBSG) and Fiber Optic Sensors (FOS), vibration-based monitoring with the use of accelerometers [3] [7], electromechanical impedance monitoring [8], and active guided waves [3] [4] [9] [10] are examples of SHM techniques used to detect damage in ship structures.

Acoustic emission (AE) is another SHM technique that is based on the recording and analysis of the transient stress waves emitted from the sudden release of energy [11] [12] due to damage initiation and growth in the material. AE has already proven to be a valuable option for the integrity assessment of different structures such as steel bridges [13] [14] [15] [16], large offshore structures [17] [18] [14] [19], and pipelines [20]. When applied to thin-walled structures, such as ship hulls, AE can cover large areas [9] with limited numbers of transducers. It is sensitive to initiation and propagation of different damage types and it is a passive method, meaning that no external excitation is needed. It has relatively low implementation costs and it can enable continuous monitoring, making it suitable for structural health monitoring of ship hulls/structures.

It is believed that the potential of AE has not yet been fully realised for ship structures. The limited use of AE monitoring in ship structures is partly due to the fact that some of the complexities in the AE signals and background noise have not yet been sufficiently understood or accounted for. In ship hulls composed of thin-walled structural components, AE waves propagate as complex multimodal dispersive ultrasonic-guided waves [21]. Structural elements such as stiffeners influence and additionally complicate wave propagation. For accurate fatigue crack detection via AE, it is crucial to understand how ultrasound waves interact with structural members and how they may affect the detection limit of damage.

The objective of this paper is to understand the guided wave propagation from damage source to AE sensors, analysing the interactions between waves and structural elements (**Fig. 1**). This investigation can potentially allow to maximize the coverage and efficiency of AE monitoring for ship structures. The approach followed comprises both experimental and numerical investigations using simulated AE sources. Next to the experimental investigation, numerical simulations using 3D Spectral Finite Element Method (SEM) have been carried out to validate and extend the results to a wider range of scenarios.

In Section 1, the methodology will be presented. Section 2 will dig into the specifics of the experimental set-up, while Section 3 will present the results and discussions. Section 4 will include the conclusions.
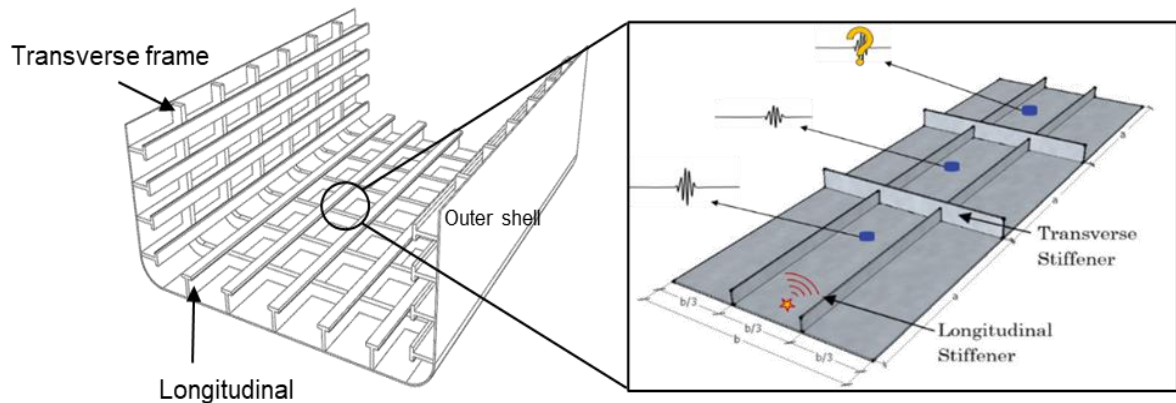

Fig. 1. : Acoustic Emission monitoring of a ship hull.

1. Methodology

1.1 Transmission coefficient expression

In thin-walled structures, damage-induced AE signals propagate as guided waves. They propagate in multiple co-existing modes at different speeds [22]. Given an acoustic emission source S, which travels through a medium W, the measured signal P at sensor can be expressed in the frequency domain as the superposition of different modes (**Fig. 2** left), plus a noise component N, with the following expression [23]:

$$P = \sum_i DWS + N \qquad (1)$$

More specifically, D represents the transfer function of the sensor while W is the transfer function of the medium through which the wave mode i is propagating.
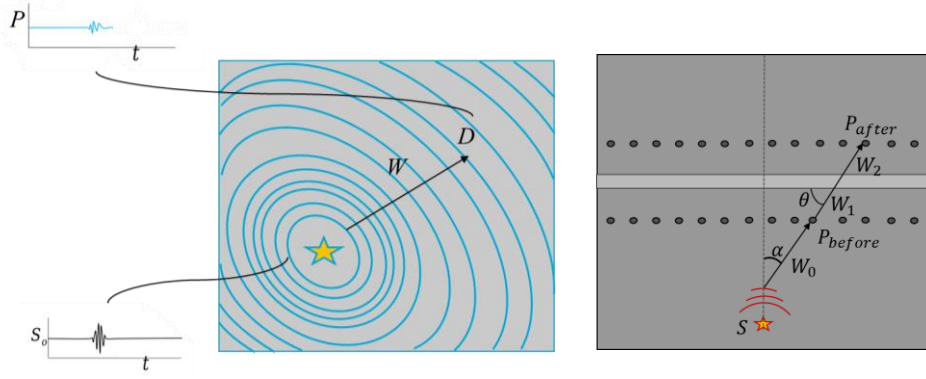

Fig. 2.*:* Damage-induced elastic wave emissions in steel plate (left); Stiffened steel plate scheme (right)

When incoming waves hit a stiffener, they lose part of their strength after the incidence as described below for an arbitrary wave mode:

$$\frac{P_{after}}{P_{before}} = \frac{D\,W_2 T(\alpha) W_1 W_0 S(\alpha)}{D\,W_0 S(\alpha)} = W_2\,T(\alpha) W_1 \qquad (2)$$

P_{before} is the signal measured before it hits the stiffener while P_{after} represents the signal measured on the other side of the stiffener. In this equation W_2, W_1, W_0 are the medium transfer functions, the source S is a function of the angle α, which is the angle of incidence of the wave with respect to the stiffener, and $T(\alpha)$ represents the angle-dependent transmission coefficient.

In this paper, an estimation of the transmission coefficient T for different angles of incidence has been carried out combining experimental results and mathematical simulations. The experimental set-up consists of a stiffened steel plate instrumented with piezoelectric sensors and will be described in Experiments.

1.2 SEM simulations

To assess and extend the results from the experimental set-up to a wider range of scenarios, 3D Spectral Finite Element Method (SEM) simulations have been carried out [24] [25]. The geometry consists of a 700x250x10 mm^3 steel plate with a vertical stiffener of 10 mm. The height of the stiffener is 110 mm. The applied loading is a 3-cycle 150kHz pulse. The source has been applied in the y-direction through the thickness of the plate to excite only A0 waves. The exact coordinates of the location are x = 250 mm, y = 5 mm, z = 250 mm; see **Fig. *3*** (yellow circle). The order of the SEM basis functions in all directions is 2, the element size

is 5 mm in x and z directions, 10 mm in the y direction, and the time step for the time integration is 0.005 µs.
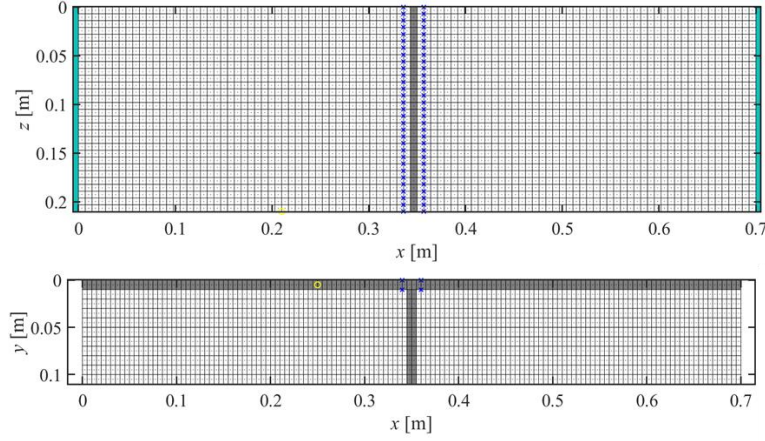

Fig. 3.: SEM model geometry

Four arrays of sensors have been placed on both sides of the plate and both sides of the stiffener to capture angles of incidence from 90 to 155 degrees. The distance of the arrays from the stiffener is 5 mm. Further details about SEM can be found in [25] [24].

2. Experiments

The experimental set-up shown in **Fig. 4** was designed to be representative of part of the inner structure of a ship. The base plate is a 1700x1200x10 mm^3 S355 steel plate. The stiffener is a 7 mm thick bulb-profile and it intersects with a longitudinal flange of 8 mm thickness. Pairs of R15α resonant piezoelectric sensors were placed on each side of the plate and of the stiffener (4 sensors in total) to record the incoming and transmitted waves excited through pencil lead breaks (PLBs). The selected sensor frequency is considered to be able to cover the representative range of frequencies for fatigue crack AE [26] i.e. 100-200 kHz. During the experiments, the sensors were placed in five different positions to measure waves at different incident angles with respect to the stiffener. The geometry is shown in **Fig. 5**. R1 is the first receiver which was moved from position 1 to position 5 following the source location. R2 is the second receiver which was kept fixed throughout the entire experiment.
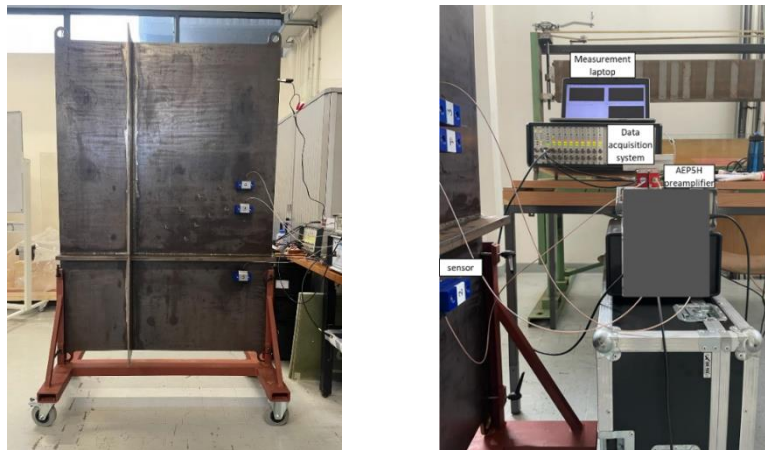

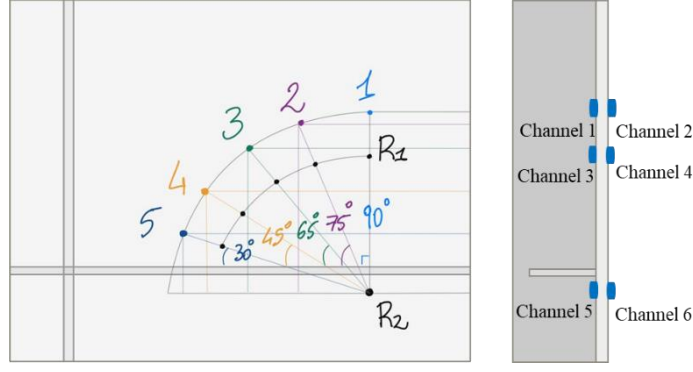**Fig. 4**.: Experimental set-up. Instrumentation close-up (right).

Fig. 5. : Sensor layout: front view (left), side view (right).

3. Results and discussion

For the considered plate thickness and frequency range, ultrasonic-guided waves propagate with two wave modes [21], the fundamental symmetric wave mode *S0* and the fundamental antisymmetric wave mode *A0*. During the experimental investigation, the piezoelectric sensors have proven to be more sensitive to out-of-plane displacement and therefore for both the experimental and the numerical investigations, the amplitude of the first antisymmetric wave mode *A0* is analysed.

In the experimental set-up, the two receivers placed before the stiffener on both sides of the plate (corresponding to channels 3 and 4 as shown in **Fig. 5**) are moved from locations 1 to 5, where the angles of incidence were respectively 90, 75, 65, 45, and 30 degrees. Five pencil lead breaks per location have been performed to excite the waves. The recorded average amplitudes for the *A0* mode per channel and location are shown in **Fig. 6**. The standard deviation of the channels represents the variability of the source due to the pencil lead breaks. For channels 3 and 4 additional variability due to the coupling is present.

The differences between the amplitudes measured by the coupled sensors (channels 3-4 and channels 5-6) seem to be mainly due to the influence of the sensors transfer function, indicated by *D* in Equation (1).
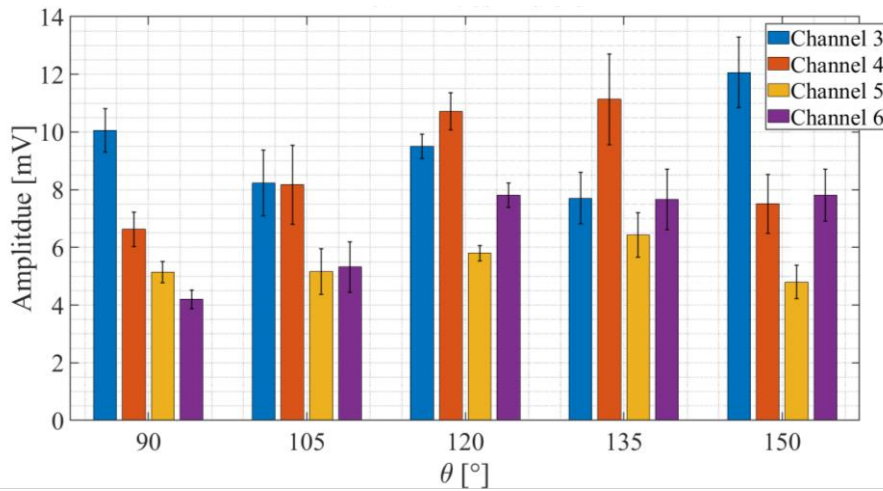

Fig. 6.: Mean and standard deviation of pencil lead breaks for all five different sensor locations.

For the numerical simulations, the amplitudes of the *A0* mode have been calculated by looking at the out-of-plane displacement v as $1/2\,(v_{top} + v_{bot})$, where v_{top} and v_{bot} are

measured for each sensor vector before and after the stiffener, on the top and bottom side of the plate. The transmission coefficient for different angles is then computed as the ratio between the amplitude after and before the stiffener. In this case, differently from the experiments, there is no variability due to coupling or source variation. The results of the transmission coefficient are shown in **Fig. 7**.
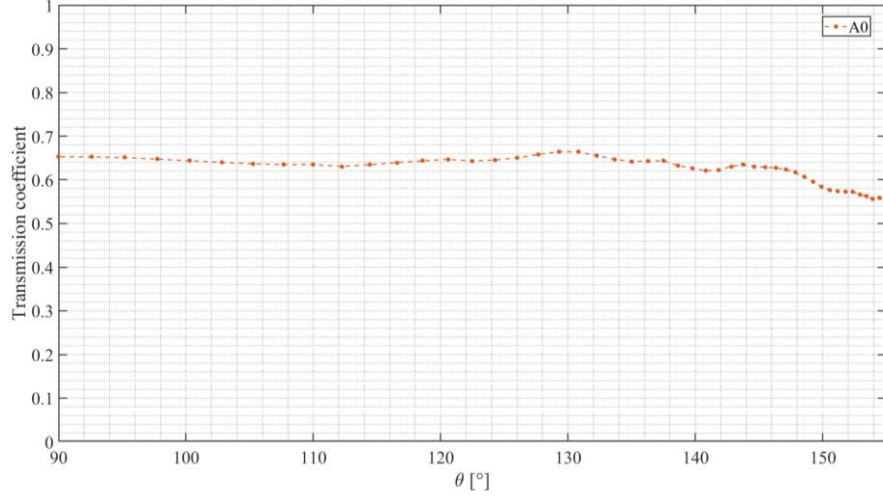

Fig. 7.: Transmission coefficient for A0 mode as a function of different angles of incidence.

To allow for comparison between the results, the transmission coefficient obtained from the SEM simulations and the experimental investigations presented in **Fig. 7** has been normalised with respect to their value for normal incidence (90 degrees). For the experimental results, due to the observed influence of the sensor transfer functions and the coupling variability on the amplitude values within the same positions, only the values measured on the top surface after the stiffener have been taken into account. The values have been then normalised with respect to the amplitude measured at normal incidence.
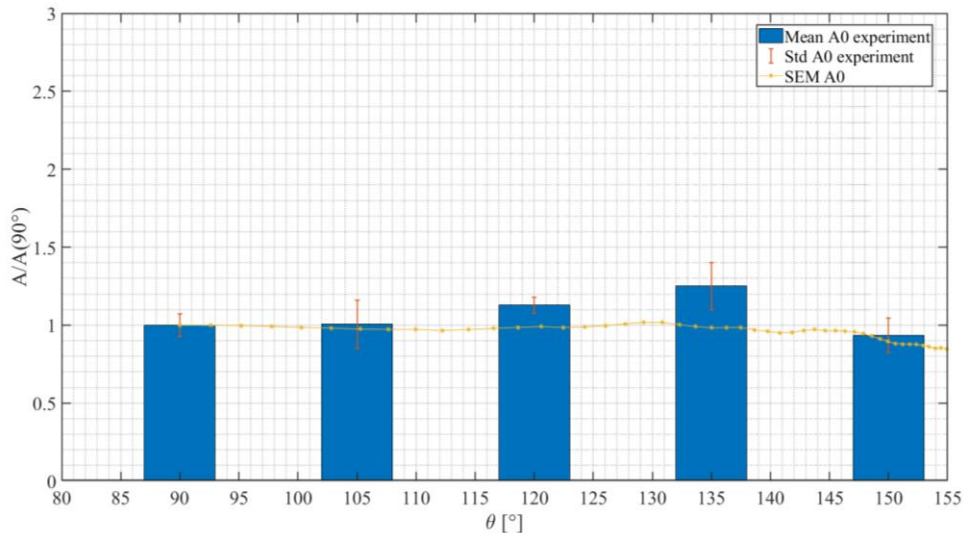

Fig. 8.: Normalized transmission of AE signals through stiffener for different angles of incidence.

By normalising the results, no geometrical spreading correction is needed. The amplitudes measured during the experimental investigation by one sensor show agreement with the SEM values for three out of five angles. The results suggest a relatively stable trend of the transmission coefficient for different incident angles from 90 to 130 degrees according to SEM and to 120 degrees according to the experimental data, after which the values start

to decrease. Experimental results show the existence of outliers with respect to the trend possibly due to the influence of angle dependence of the transducers and source variation (to be investigated in the future research). The differences between numerical and experimental results may also be partly due to the different thicknesses of the stiffeners.

A transmission coefficient of 0.65 (as shown in **Fig. *7***) implies an amplitude drop of about 4 dB of the signal after encountering one stiffener. To exemplify, assuming a damage induced AE signal of 95 dB at the source, after hitting one stiffener with an angle from 90 to 130 degrees, it would have an amplitude of around 91 dB. Considering *n*-stiffeners, the total amplitude drop would be of 5*n* dB. Taking into account a background noise of at least 50 dB in marine operational environment, the AE signal can span over more than five consecutive stiffeners and still be recorded with an amplitude above the noise threshold. If the spacing between stiffeners is considered to be less than 600 mm [27], the necessary distance between the source and the receiver for it to be recorded would be approximately 1.2 m.

4. Conclusions

In this paper, the influence of stiffeners on the AE signals for AE monitoring of ship structures was investigated. The combination of experimental and numerical results suggests that an AE signal released from a typical fatigue damage source in a ship hull structure can be successfully recorded with 150 kHz resonant piezoelectric sensors with an amplitude drop of about 5 dB per stiffener for incident angles of 90-130 degrees.

The results of this study can be used as a starting point to maximize the coverage of AE monitoring systems and enhance their sensitivity for the detection of fatigue cracks on ship structures taking into account the presence of multiple stiffeners. More investigation has to be carried out to cover the influence of different excitation frequencies and different wave modes.

5. Acknowledgements

References

[1] R. Hageman, *Uncertainty quantification of fatigue design loads when compared with in-service,* 2022.

[2] R. A. Votsis, C. Michailides, E. A. Tantele and T. Onoufriou, "Review of Technologies for Monitoring the Performance of Marine Structures," in *International Ocean and Polar Engineering Conference*, 2018.

[3] J. Zhang, W.-H. Kang, K. Sun and F. Liu, "Reliability-Based Serviceability Limit State Design of a Jacket Substructure for an Offshore Wind Turbine," *energies ,* 2019.

[4] Committee V.7, "ISSC report," 2022.

[5] M. G. R. Sause and E. Jasiūnienė, Eds., Structural Health Monitoring Damage Detection Systems for Aerospace, 2021.

[6] A. Silva-Campillo, F. Pérez-Arribas and J. C. Suárez-Bermejo, "Health-Monitoring Systems for Marine Structures: A Review," *sensors,* 2023.

[7] B. Bayik, P. Omenzetter, D. van Der A and Pavlovskaia, "Comparison of damage sensitivities of autoregressive coefficients and natural frequencies for structural health monitoring of a top tensioned riser," in *EWSHM*, 2018.

[8] M. Winklberger, C. Kralovec, P. Heftberger and M. Schagerl, "Monitoring growing cracks in aircraft lugs by means of the electro-mechanical impedance method," *Procedia Structural Integrity,* 2022.

[9] S. Shoja, V. Berbyuk and S. Mustapha, "Design optimization of transducer arrays for uniform distribution of guided wave energy in arbitrarily shaped domains," *Ultrasonics,* 2020.

[10] L. Pahlavan and G. Blacquière, "Fatigue crack sizing in steel bridge decks using ultrasonic guided waves," *NDT&E International,* 2015.

[11] N. H. Faisal, M. G. Droubi and J. A. Steel, "Corrosion monitoring of offshore structures using acoustic emission sensors," *A journal of the Institute of Corrosion,* 2017.

[12] ASTM International , *E1316-13c Standard Terminology for Nondestructive Examinations,* 2013.

[13] A. Nair and C. Cai, "Acoustic emission monitoring of bridges: Review and case studies," *Engineering Structures,* 2008.

[14] C. Grosse, "Acoustic emission localization methods for large structures based on beamforming and array techniques," *Non-Destructive Testing in Civil Engineering,* 2009.

[15] G. C. McLaskey, S. D. Glaser and C. U. Grosse, "Beamforming array techniques for acoustic emission monitoring of large concrete structures," *Journal of Sound and Vibration,* 2010.

[16] P. L. Pahlavan, J. Paulissen, R. Pijpers, H. Hakkesteegt and R. Jansen, *Acoustic Emission Health Monitoring of Steel Bridges,* Nantes, France: EWSHM - 7th European Workshop on Structural Health Monitoring, 2014.

[17] S. Alkhateeb, F. Riccioli, F. Morales and L. Pahlavan, "Non-Contact Acoustic Emission Monitoring of Corrosion under Marine Growth," *Sensors,* 2023.

[18] F. Riccioli and P. Pahlavan, "NON-CONTACT ACOUSTIC EMISSION MONITORING OF CORROSION-FATIGUE DAMAGE IN SUBMERGED STEEL STRUCTURES," in *International Workshop on Structural Health Monitoring (IWSHM)*, Stanford, 2023.

[19] J. Mitchell and L. Rogers, "Monitoring Structural Integrity of North Sea Production Platforms by Acoustic Emission," 1992.

[20] N. Ullah, Z. Ahmed and J.-M. Kim, "Pipeline Leakage Detection Using Acoustic Emission and Machine Learning Algorithms," *Sensors,* 2023.

[21] V. Giurgiutiu, Structural health monitoring with piezoelectric wafer active sensors, 2008.

[22] M. Adams, A. Huijer, C. Kassapoglou, J. Vaders and L. Pahlavan, "In Situ Non-Destructive Stiffness Assessment of Fiber Reinforced Composite Plates Using Ultrasonic Guided Waves," *Sensors,* no. Acoustic and Ultrasonic Sensing Technology in Non-destructive Testing, 2024.

[23] B. Scheeren, M. L. Kaminski and L. Pahlavan, "Acoustic emission monitoring of naturally developed damage in large-scale low-speed roller bearings," *Structural Health Monitoring,* 2023.

[24] L. Pahlavan, *Wave Propagation in Thin-walled Composite Structures: Application to Structural Health Monitoring,* 2012.

[25] L. Pahlavan, C. Kassapoglou and Z. Gürdal, "Spectral formulation of finite element methods using Daubechies compactly-supported wavelets for elastic wave propagation simulation," *Wave Motion,* 2013.

[26] M. Chai, C. Lai, W. Xu, Q. Duan, Z. Zhang and Y. Song, "Characterization of Fatigue Crack Growth Based on Acoustic Emission Multi-Parameter Analysis," *materials,* 2022.

[27] Bureau Veritas, *HULL STRUCTURE AND ARRANGEMENT FOR THE CLASSIFICATION OF CARGO SHIPS LESS THAN 65 M AND NON CARGO SHIPS LESS THAN 90 M,* 2022.